



Calhoun: The NPS Institutional Archive
DSpace Repository

Theses and Dissertations

1. Thesis and Dissertation Collection, all items

1955

Photoelastic study of pressure vessel stresses.

Burke, Robert E.

Massachusetts Institute of Technology

<http://hdl.handle.net/10945/14492>

Downloaded from NPS Archive: Calhoun



Calhoun is the Naval Postgraduate School's public access digital repository for research materials and institutional publications created by the NPS community. Calhoun is named for Professor of Mathematics Guy K. Calhoun, NPS's first appointed -- and published -- scholarly author.

Dudley Knox Library / Naval Postgraduate School
411 Dyer Road / 1 University Circle
Monterey, California USA 93943

<http://www.nps.edu/library>

PHOTOELASTIC STUDY OF PRESSURE VESSEL STRESSES

ROBERT EUGENE BURKE

Library
U. S. Naval Postgraduate School
Monterey, California

1-14

PHL - PHOTOELASTICITY

PRE - PRESSURE

STR - STRESSES

Perry G. Davis **BOOKBINDING**

2216 CLEMENT STREET San Francisco 21, Calif. BA. 1-6352

DIRECTIONS FOR BINDING

BUCKRAM

COLOR NO. 8854

FABRIKOID

COLOR _____

LEATHER

COLOR _____

Letter in Gold

OTHER INSTRUCTIONS

Letter on front cover:

PHOTOELASTIC STUDY OF PRESSURE

VESSEL STRESSES

ROBERT E. BURKE

LETTERING ON BACK
TO BE EXACTLY AS
PRINTED HERE.

BURKE

1955

THESIS
B8836

PHOTOELASTIC STUDY OF PRESSURE VESSEL STRESSES

by

Robert Eugene Burke

Lieutenant, United States Navy

Submitted in partial fulfillment
of the requirements
for the degree of
MASTER OF SCIENCE
IN
MECHANICAL ENGINEERING

United States Naval Postgraduate School
Monterey, California

1 9 5 5

Thesis

38836

PREFACE

The work reported in this thesis was performed at the United States Naval Postgraduate School, Monterey, California, during the academic year 1954-1955, as part of the requirements for the degree of Master of Science in Mechanical Engineering.

The writer wishes to express his appreciation to Professors John E. Brock and Robert E. Newton for their guidance and technical assistance, Mr. Reuel P. Kennicott for his assistance in the machining and fabrication of the models, and to his wife for her understanding and patience without which this thesis could not have been completed.

TABLE OF CONTENTS

Item	Title	Page
Chapter I	Introduction	1
	Summary	1
	Properties of Armstrong's C-9 Adhesive	3
	The Problem of the Tee Connection	4
	Three-Dimensional Photoelasticity	5
	Material Selection	6
Chapter II	Mechanical and Optical Properties of Armstrong's C-9 Adhesive	7
Chapter III	Fabrication of Models	19
	Casting	19
	Cementability	23
	Machining	25
	Difficulties Encountered	26
Chapter IV	Test Set-Up and Procedure	34
Chapter V	Test Results	41
	Slicing	41
	Interpretive Procedures	41
	Static Checks	42
	Why the Complete Solution Was Not Attained	43
Bibliography	49
Appendix I	Mechanical Properties Data	50
Appendix II	Computation Data	55
Appendix III	Additional Data	57

LIST OF ILLUSTRATIONS

Figure		Page
1.	Room Temperature Stress-Strain Diagram	10
2.	Variation of Modulus of Elasticity With Temperature . .	11
3.	Room Temperature Stress-Optic Constant Calibration . . .	12
4.	Creep Test at 76° C	13
5.	Tensile Specimens Used in Stress-Strain Curves	14
6.	High Temperature Creep Machine	15
7.	Pure Bending Specimens	16
8.	Pure Bending Jig and Specimen	17
9.	Frozen Stress Pattern for Pure Bending	18
10.	Plastic Components	20
11.	Header and Branch of Third Tee Prior to Cementing . . .	27
12.	Third Tee After Cementing	28
13.	Stress Pattern of a Circular Disk Under Load	29
14.	Stress Pattern of a Cemented Circular Disk Under Load	30
15.	Frozen Stress Pattern of a Cemented Joint	31
16.	Details of Third Tee	32
17.	Similarity of Cemented Joint to a Welded Joint	33
18.	Stress Freezing Apparatus	35
19.	Blanking Off the Ends of the Third Tee	36
20.	Third Tee Blanked Off and Ready for Testing	37
21.	Arrangement of Tee in the Oven	38
22.	Stress Freezing Heating and Cooling Cycle	39
23.	Test Set-Up for Third Tee	40

LIST OF ILLUSTRATIONS

Figure		Page
24.	Polariscope Used in Analyzing Frozen Stress Patterns . .	44
25.	Partial View of Centerline Slice Used to Determine Longitudinal Boundary Stresses in Branch	45
26.	Partial View of Centerline Slice Used to Determine Longitudinal Boundary Stresses in Header	46
27.	Plot of σ_z on Inner and Outer Surfaces Along Centerline of Branch	47
28.	Plot of σ_z on Inner and Outer Surfaces Along Centerline of Header	48

TABLE OF SYMBOLS

(Listed in the order of their use in the text)

f	- Material Stress-Optic Constant, psi/in/fringe
E	- Modulus of Elasticity, psi
ϵ	- Strain, in/in
σ	- Normal Stress, psi
δ	- Elongation, in
n	- Fringe Order at any Point
h	- Height of Bending Specimens, in
t	- Bending and Tensile Specimen Thickness, in
M	- Bending Moment, inch-lbs
σ_z	- Longitudinal Stress, psi
σ_r	- Radial Stress, psi
F	- Model Stress-Optic Constant, psi/fringe
z'	- Distances from Inner Surfaces of Model (measured on photographs) to a Point Being Analyzed, in
w	- Thickness of Slice, in

CHAPTER I

INTRODUCTION

1. Summary.

The content of this thesis is briefly summarized in the following abstract:

ABSTRACT

The investigation described in this thesis was undertaken to study the feasibility of determining the stress distribution in piping branch connections by the use of three-dimensional photoelasticity using the stress freezing technique. One of the principal problems anticipated and actually encountered was that of obtaining suitable photoelastic models. It developed that no other agency, laboratory, or group was prepared to produce such models for this investigation, and it became necessary to produce the models at this activity. This necessity was seized as the opportunity to investigate the photoelastic properties of a new class of resins (the epoxy group) and to develop techniques of casting and fabricating this material so as to form the desired models. Development of these techniques proved to be so time consuming that it was not possible to perform a complete stress analysis of a piping branch connection model. However, a partial analysis was completed and the results of this partial analysis were subjected to a static check which sub-

stantiates the validity of the process of experimentation and analysis. Sufficient model "slices" were photographed to assure that good, clear isochromatic patterns could be obtained to provide for a complete analysis of such structures.

The following conclusions appear to be warranted:

- (a) It is feasible to investigate the stresses in piping branch connections by the use of three-dimensional photoelasticity using the stress freezing technique and employing models cast and fabricated using an epoxy resin as described herein.
- (b) The techniques of producing such models are not easily mastered and in future investigations sufficient time should be allowed to permit the investigator to master the necessary techniques.
- (c) Armstrong's C-9 adhesive, an epoxy resin, is an excellent photoelastic material, having a figure of merit of approximately 1200.

The properties of this material are summarized in part 2 of this introduction. It is pertinent to discuss the practical importance of the problem of determining the stress distribution in piping branch connections and this is done briefly in part 3 of this introduction. Part 4 of the introduction discusses briefly the principles underlying three-dimensional photoelasticity using stress freezing and traces recent

development of materials for this purpose. Part 5 of the introduction discusses briefly the problem of obtaining models for this investigation and of the decision to produce the models at this activity employing a new photoelastic material, Armstrong's C-9 adhesive.

2. Properties of Armstrong's C-9 Adhesive.

The investigation described in this paper showed Armstrong's C-9 adhesive to be an excellent three-dimensional photoelastic material having the following properties:

Critical temperature	176°F
f in psi per inch per fringe	
room temperature (tension)	72.0
room temperature (pure bending)	70.6
effective (pure bending - frozen)	1.31
E in psi	
room temperature	527,500
critical	1,600 (approx.)
Figure of merit (see page 8)	1,220 (approx.)

This material is obtainable in a two component liquid form from which suitable three dimensional models may be prepared. It may be cast in inexpensive molds but requires considerable technique to produce a casting free of soft spots and/or bubbles. Other characteristics which are noteworthy in the evaluation are:

- (a) Its ability to be easily and quickly cured.
- (b) Its excellent cementability with attendant good tensile strength and negligible distortion of stress pattern.
- (c) Its very good machining properties.

(d) It is easy to anneal for removing casting and machining stresses.

(e) It requires less time for the stress freezing than is the case with many other materials since a more rapid cooling rate may be used without adverse effects of craze marks or cracking.

3. The Problem of Tee or Nozzle Connection in Piping and Pressure Vessel Work.

Tee or nozzle connections are present in almost all piping systems and pressure vessels. The tee connection in most of its applications is subjected to an internal pressure loading. The discontinuity arising at the junction of the branch and header of a tee connection obviously alters the stress distribution as determined by elementary theory for bodies of revolution. The solution of the complete stress distribution of a tee connection due to internal pressure has not to date been obtained experimentally or theoretically.

In the fabrication of a tee connection the removal of material so as to make the opening causes a reduction in the tensile load carrying capacity. Present design criteria are based on the principles of reinforcing the opening to replace an equivalent amount of tensile load carrying capacity. Detailed instructions for this procedure are given [1, 2, 3]¹ to assure satisfactory service for a tee connection subjected to internal pressure. However, it is not known to what extent criteria of this type assure safety for all cases by requiring uneconomic design

1. Numbers in brackets refer to the bibliography.



in certain cases, or even that these criteria do indeed assure safety in these connections commensurate with the safety incorporated in other components of the piping system. Accordingly, it is evident that any light which can be shed on the actual distribution of stresses in such connections will be of assistance in the evolution of better and more economic design criteria. It is this thought which has provided the basic motivation of the present investigation.

4. Three-Dimensional Photoelasticity.

When a model prepared from a suitable photoelastic material is heated to a critical temperature range and loaded, it has the property of assuming the elastic state of stress consistent with the loading, shape, and the mechanical properties of the material. The truly remarkable feature of this phenomenon is that if the model is slowly cooled while the loading is maintained constant, at room temperature the model has retained this stress system. If the model is then sliced in appropriate planes these slices may be examined as two-dimensional specimens. Thus by judicious choice of slices the experimenter has the capability of obtaining the three-dimensional stress distribution [4, 5, 6].

This three-dimensional photoelasticity is known as stress freezing and it has been demonstrated that these frozen stresses are typical of the elastic state of stress.

The development of three-dimensional photoelasticity has moved forward with the development of Fosterite [7] a styrenealkyd resin considered the best available material today. Smith [8] used it successfully by machining solid cylinders of it into cylindrical pressure vessels. Cost and availability are severe limitations on its use at present. Kriston



was investigated by Taylor [9] and was considered an excellent material for three-dimensional photoelasticity. However, Kriston has since been taken off the market. Frocht [10] recently reported the suitability of Castolite as a two- or three-dimensional material either through casting or cementing.

5. Material Selection.

Initially the planning was to have the models for this thesis manufactured by those engaged in the plastic business. Inquiries were sent out but from the replies it was apparent that this effort would be unsuccessful. Accordingly it was decided to include the casting and fabrication of the models in this investigation.

The decision on what particular material to use was then encountered since Kriston as mentioned earlier had been taken off the market. Mr. M. M. Leven of Westinghouse Research Laboratories² recommended either Castolite or an epoxy resin. Since the epoxy resins are so new in the field of plastics, their use in this investigation would assist in the evaluation of available and suitable materials for three-dimensional photoelasticity.

The particular material chosen is Armstrong's C-9 clear epoxy resin which is cured with activator "A." It is procurable from Armstrong Products Company, Argonne Road, Warsaw, Indiana. The prices for these components are as follows:

Resin (1 gallon)	\$23.00
Activator "A" (12 oz., appropriate amount for 1 gallon of resin)	\$ 1.00

2. Private correspondence to writer dated November 11, 1954.



CHAPTER II

MECHANICAL AND OPTICAL PROPERTIES OF ARMSTRONG'S C-9 ADHESIVE

The room temperature modulus of elasticity of Armstrong's C-9 adhesive was determined by tensile test as $.5275 \times 10^6$ psi as shown in Figure 1. The variation of the modulus of elasticity with temperature is shown in Figure 2. The modulus of elasticity at the critical temperature of 176°F was approximately 1600 psi. At room temperature the stress optical constant was determined by compression tests to be 72.0 psi/in/fringe as shown in Figure 3. The pure bending specimens mentioned in a following paragraph were also used to check the value of the stress optic constant; they afforded a value of 70.6 psi/in/fringe which checks very well with the value given above. For the room temperature value of the stress optic constant, the value of 72.0 psi/in/fringe is recommended since the compression tests results are believed to be more reliable than the pure bending test results. However, for calibration of the material at the critical temperature the pure bending test was used since the test set-up did not permit making a compression test at elevated temperatures.

The critical temperature for the stress freezing was determined by using pure bending specimens in a controlled heating bath between the polarizer and analyzer of a polariscope. As the temperature of the bath was raised the fringes were observed. It was found that the temperature range at which no additional fringes appeared was approximately 78°C to 87°C. The critical temperature was then selected as 80°C (176°F) on the basis of obtaining the increased modulus of elasticity as shown on Figure 2. As a further check a creep test was run at 76°C and the results are shown in Figure 4. Although the temperature used was slightly under the selected



critical temperature the results are indicative of the correctness of the choice of critical temperature.

The stress-strain curves of Figure 2 were obtained using tensile specimens machined from cast blanks to the desired size and shape of Figure 5. The tests were run on the high temperature creep machine shown in Figure 6 using a 14.7:1 lever ratio. The purpose of these curves was to determine the variation of modulus of elasticity with temperature and to indicate the stress level that could be applied to the tee connections under test.

The pure bending specimens used were of the type shown in Figure 7. Initially they were of one inch height; however, lateral buckling at critical temperature necessitated a decrease in this height (see Figure 7). Since the buckling is approximately proportional to this height whereas the fringe order varies inversely as the square of this height a substantial gain in fringe order was obtained without buckling. The pure bending jig and calibration specimen after stress freezing is shown in Figure 8. The frozen stress pattern for a typical pure bending specimen is shown in Figure 9. The material stress-optic constant as determined by pure bending frozen stress patterns was 1.31 psi per in per fringe.

The figure of merit is an accepted way of rating a material for its suitability in three-dimensional photoelasticity. It is defined as the ratio of the modulus of elasticity to the material stress-optic constant for the frozen patterns. The figure of merit for Armstrong's C-9 adhesive is approximately 1220. This value is approximate since the modulus of elasticity value used in determining it was the critical temperature modulus and not the frozen stress pattern modulus. With due regard to

the expected differences in these two moduli it appears that Armstrong's C-9 adhesive has a figure of merit twice that of Fosterite.



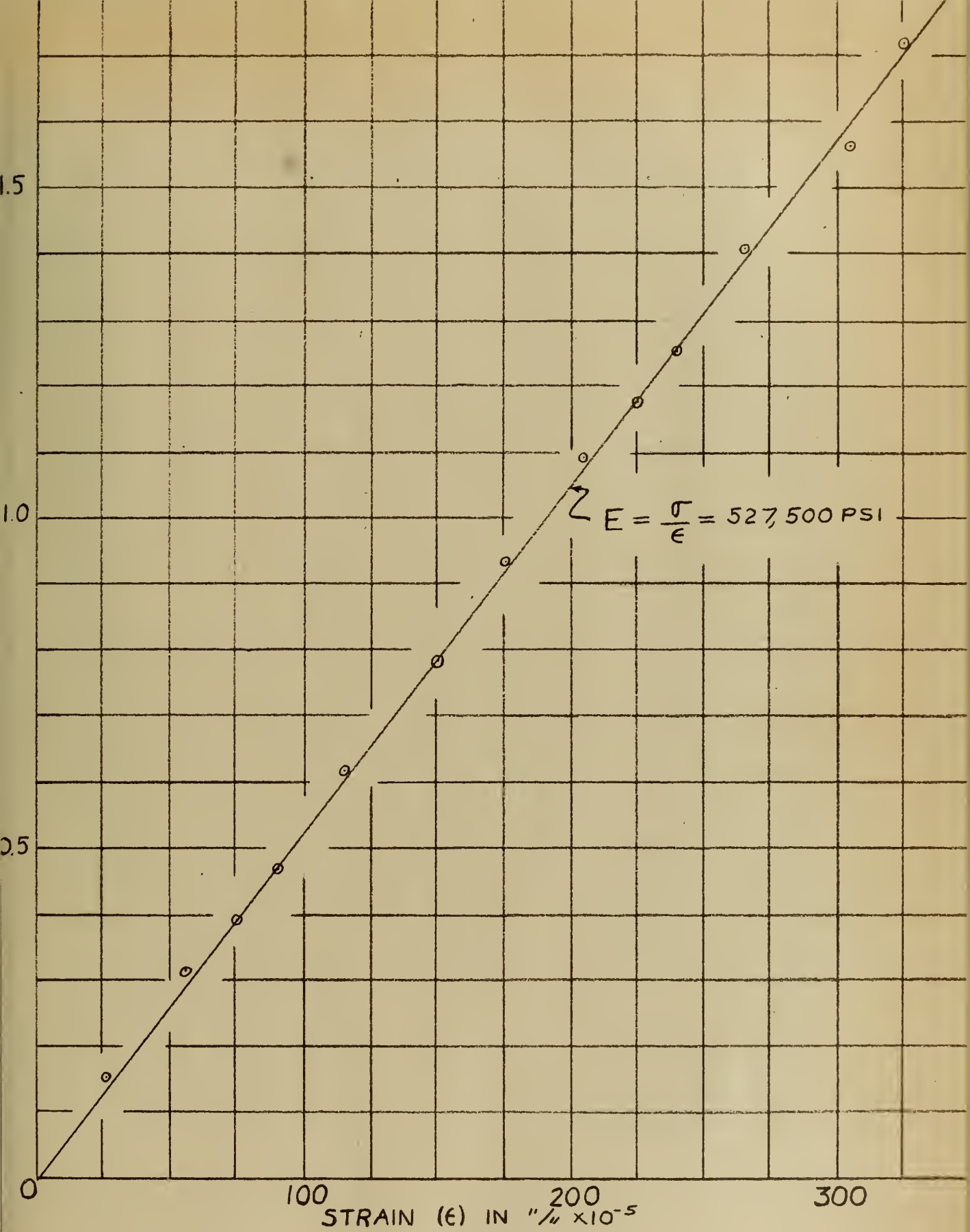


FIGURE 1. Room Temperature Stress-Strain Diagram.

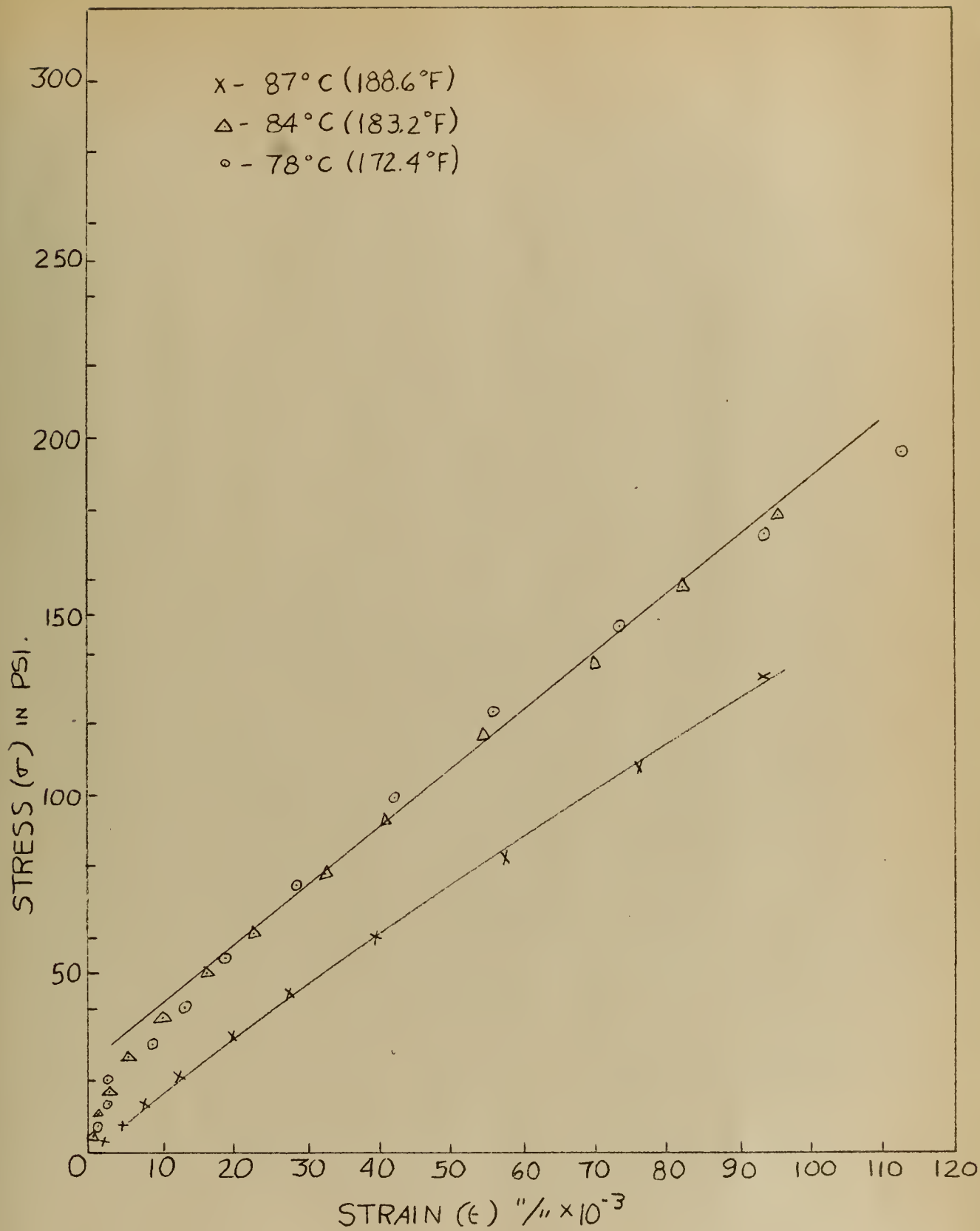


Figure 2. Variation of Modulus of Elasticity with Temperature.

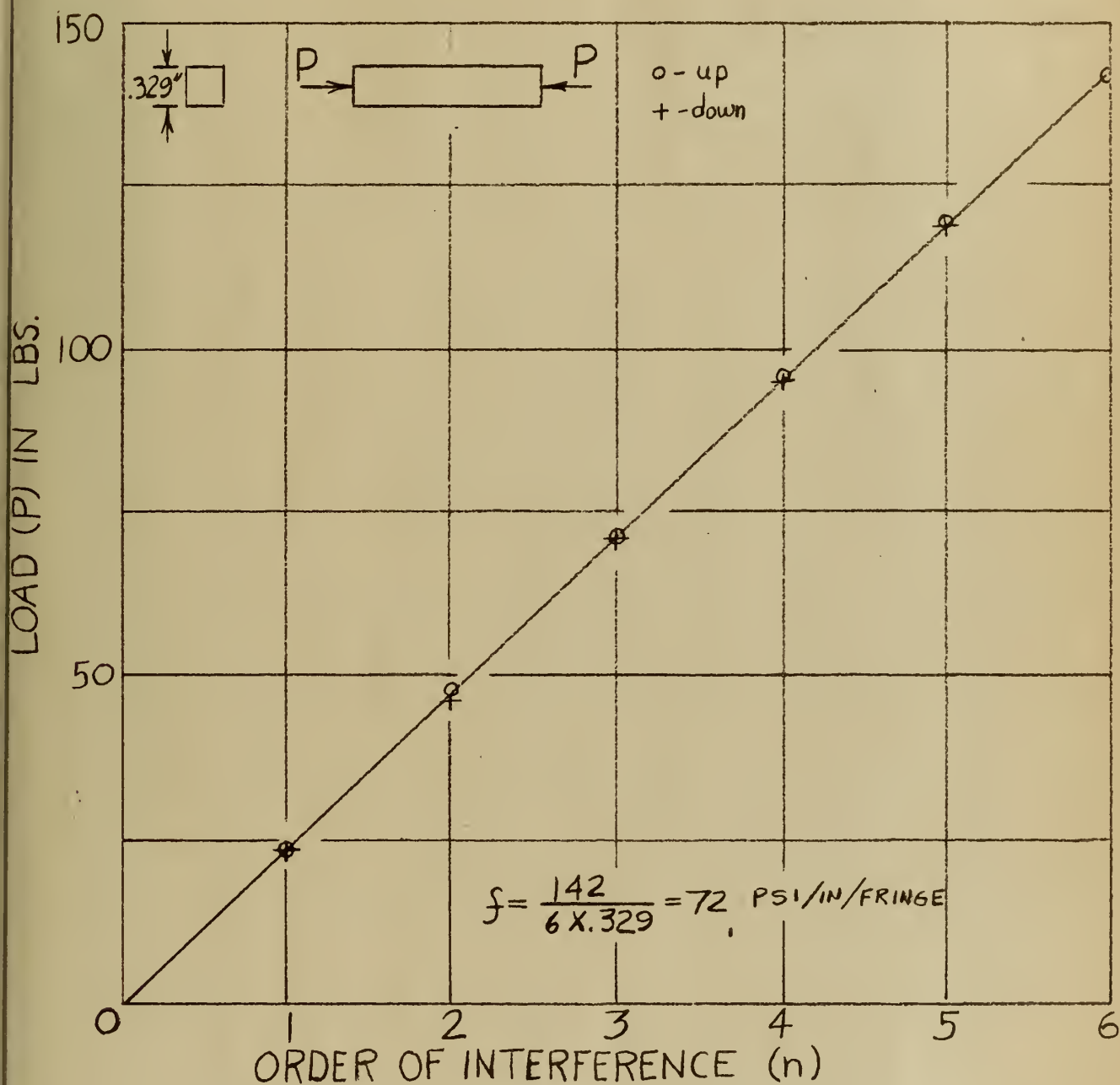


FIGURE 3. Room Temperature Stress-Optic Constant Calibration.

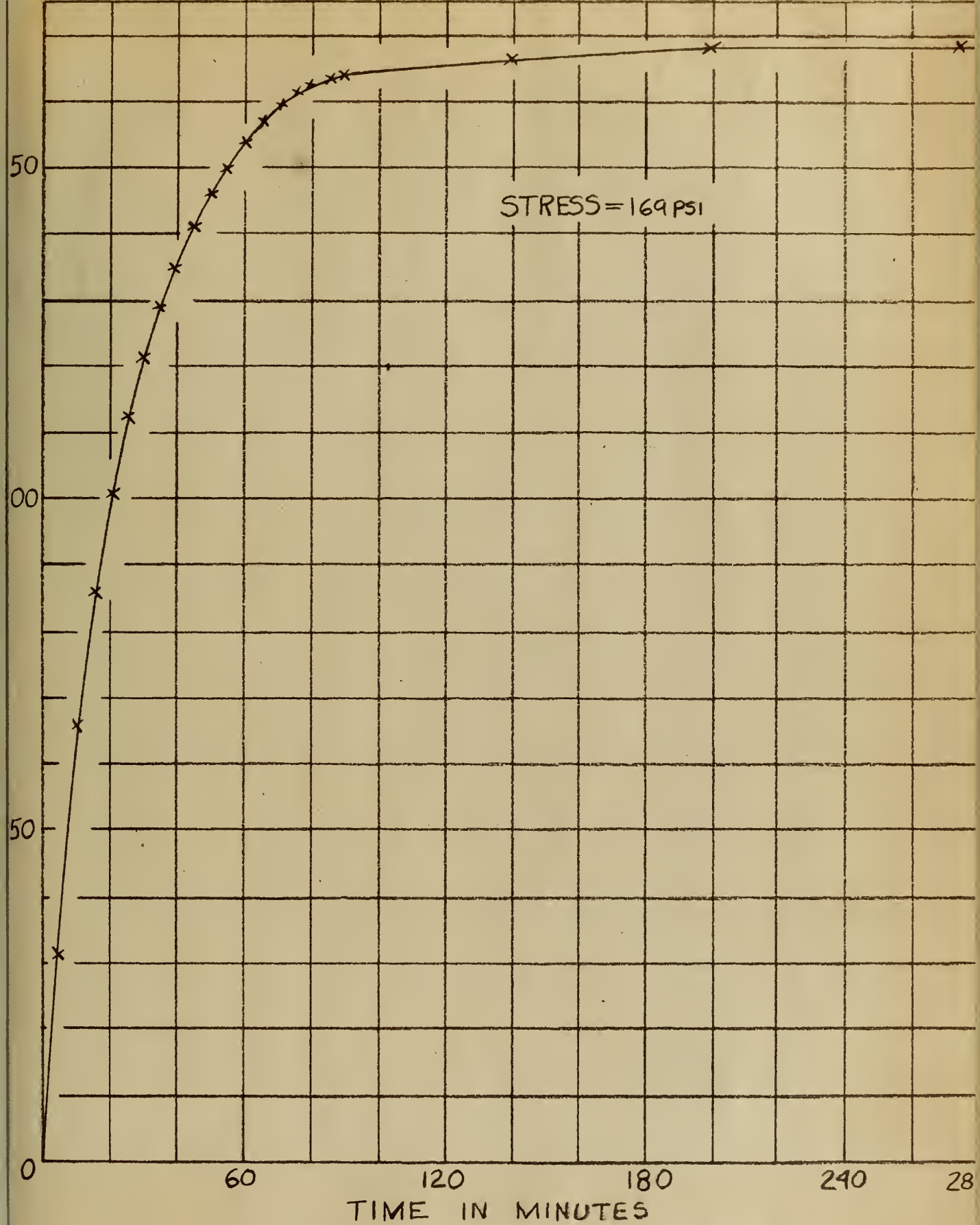


FIGURE 4. Creep Test at 76°C

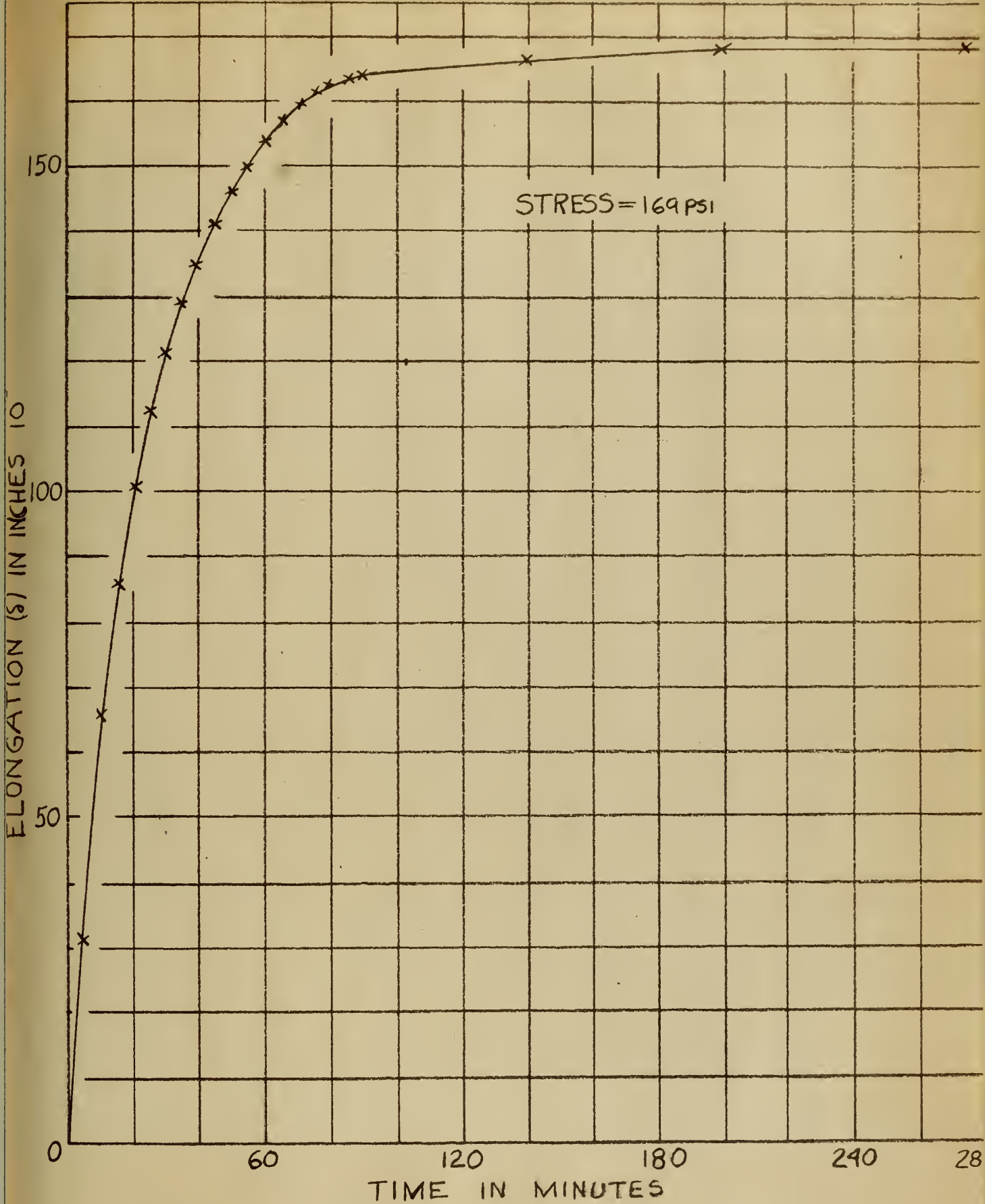


FIGURE 4. Creep Test at 76°C

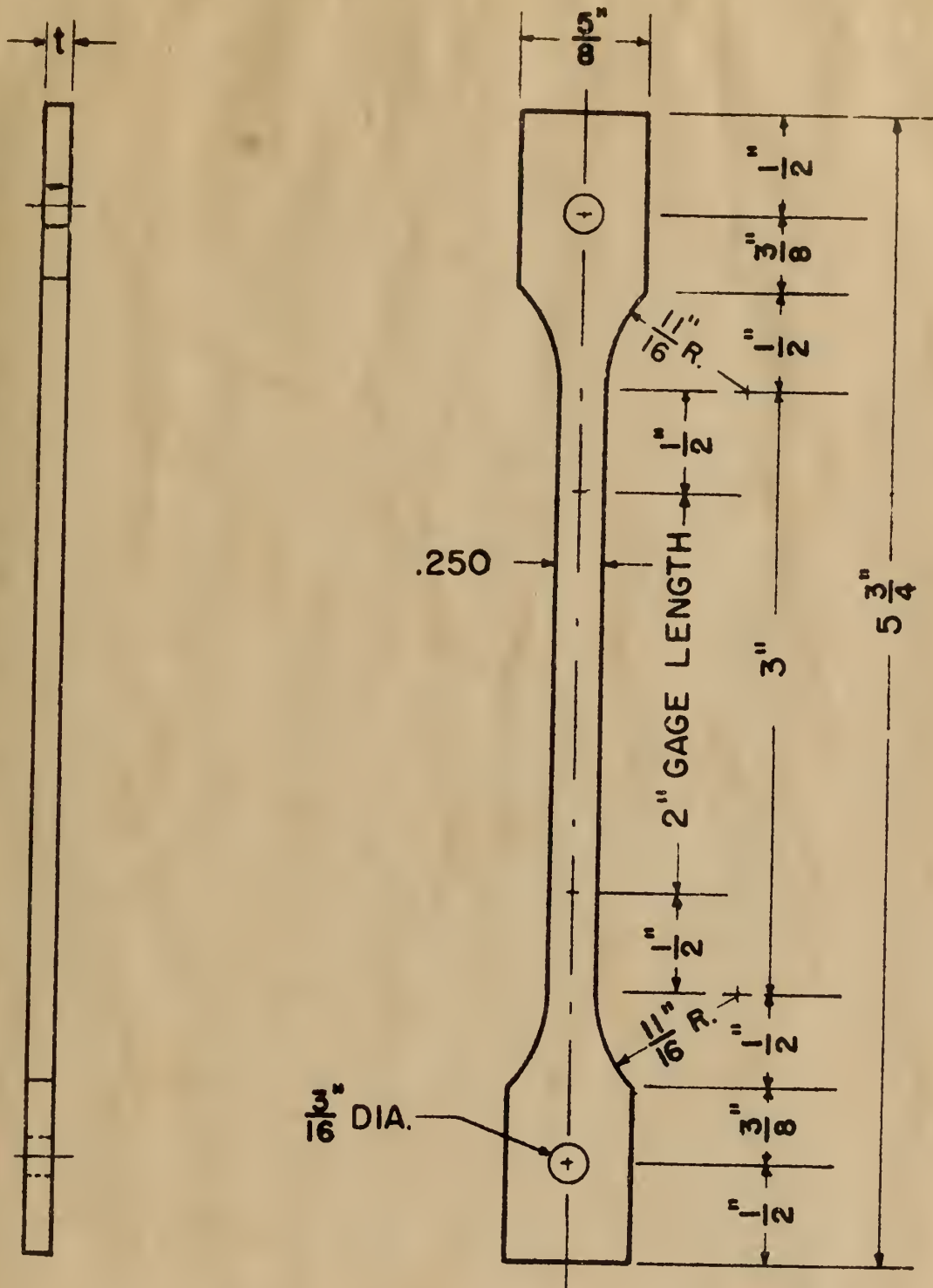


Figure 5. Tensile Specimens Used in Stress-Strain Curves.

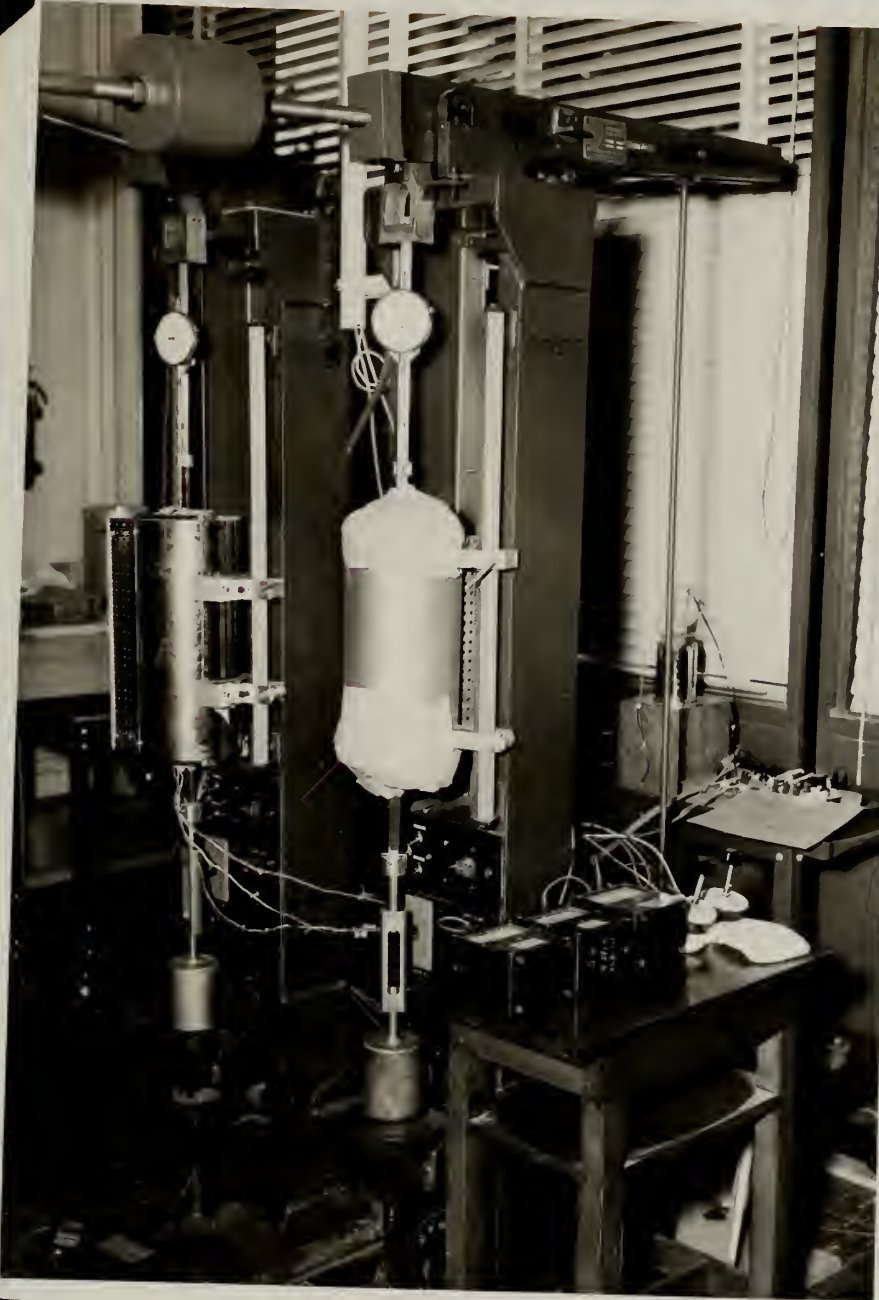


Figure 6. High Temperature Creep Machine.

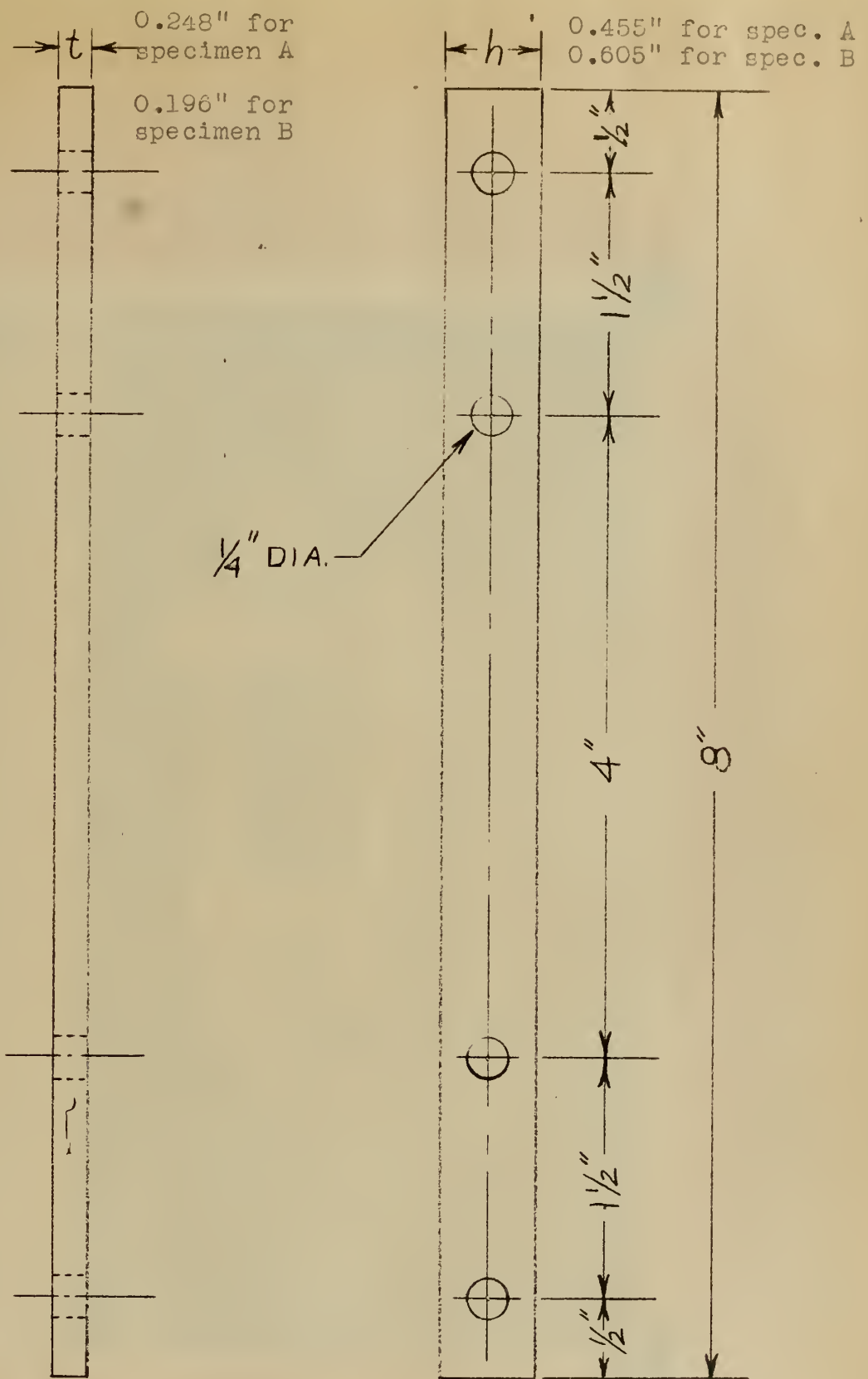


Figure 7. Pure Bending Specimen.

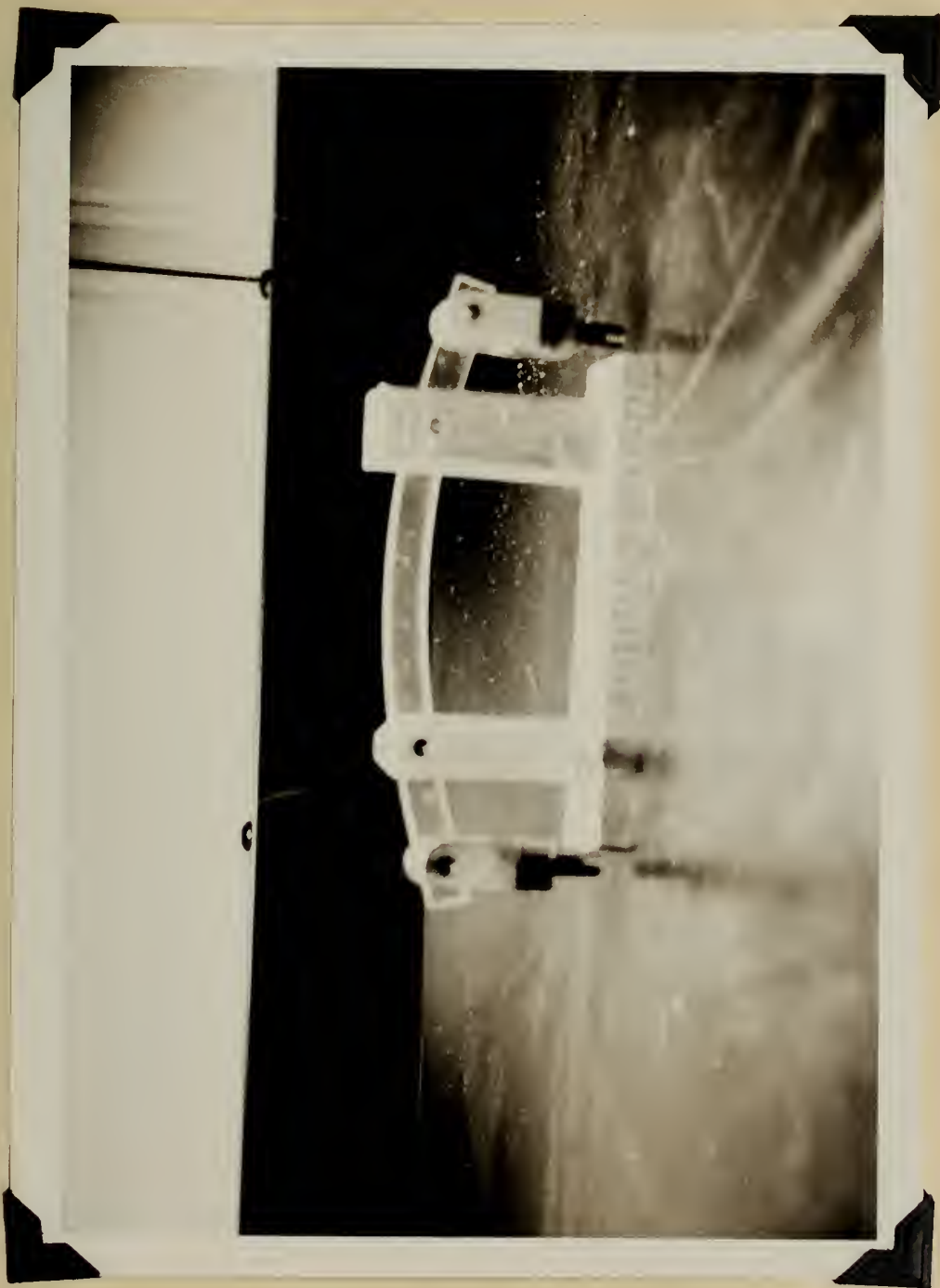
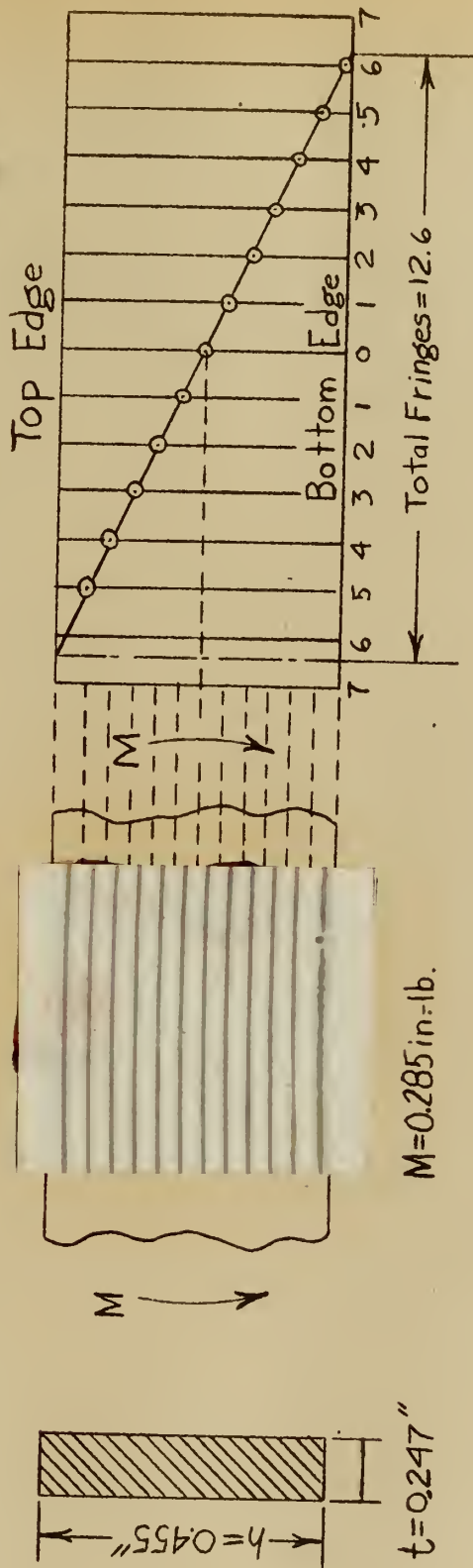


Figure 8. Pure Bending Jig and Specimen.



$$f = \frac{12 M}{n h^2} = \frac{12 \times 0.285}{12.6 (0.455)^2} = 1.31 \text{ psi/in./fringe}$$

FIGURE 9. Frozen Stress Pattern for Pure Bending.

CHAPTER III

FABRICATION OF MODELS

1. Casting.

The Armstrong C-9 adhesive is a thermo setting liquid epoxy resin. It is a two component system consisting of a syrup-like resin and a liquid activator. The plastic is formed by combining eight parts by weight of the activator to 100 parts of resin. Figure 10 shows one gallon of resin and sufficient activator for this amount. The solidification and curing is accomplished through chemical reaction either at room temperature or more rapidly at moderately elevated temperatures. The curing cycle begins as soon as the activator is mixed with the adhesive. This is evident by a gradual thickening, first to a gel stage and then by hardening. Complete curing is accomplished in about six days at room temperature or one to two hours at 165°F after hardening has taken place.

It was found that paper cups for hot liquids were the best pots for mixing the plastic. As poured from the container to the cups the resin invariably formed many bubbles. Allowing the cups then to set in sunlight for several hours generally removed most of these bubbles. After removing the bubbles the resin was weighed and the amount of activator was determined for the amount of resin. In the mixing it was found to be very difficult to maintain a bubble free and yet homogenous mixture. Gentle stirring with a glass rod could control the introduction of bubbles but it failed to provide a thorough enough mixture to prevent some unhardened spots from turning up in the casting. These unhardened or soft spots were abrupt in their beginning and ending (i.e., there



Figure 10. Plastic Components.



was no gradual transition from soft to hard structure). By tilting the cup and rotating it slowly in the fingers a good mixture was obtained. However, many tiny bubbles could not be kept from appearing. The best method found was that of pouring between two cups. The bubble free resin with activator was first gently stirred to provide a slight mixing so as to obtain a viscosity between that of the resin and activator alone. It was then gently poured from one cup to another in a manner such that it moved off the lip of one cup to the wall of the other, maintaining a continuity of mass flow. The mixture at first appears slightly cloudy and then clears as the mixing proceeds. Since the activator is volatile and vapors can be seen for some time after mixing is started, the pots were watched and after no further vapors were observed, the mixing continued for five to ten minutes to assure the thorough mixing needed.

Since the chemical reaction of hardening is exothermic, the amounts mixed at one time should not exceed about one-half pound. The amounts actually mixed in this work were held to 50 to 100 grams, necessitating a series of pours in many cases. The excellent adhesion to the previous pours and attendant nearly invisible glue line enabled this to be done. Using resin and activator originally at room temperature the effective pot life was approximately 20 minutes from the time of commencing mixing. By pouring within this time no noticeable heating of the pot occurred. However, too much delay at this stage caused the pot to heat up signalling the end of the effective pot life and castings poured at this stage were invariably brittle.

Due to the tenacity with which the hardened plastic adhered to the molds of glass, plaster of Paris, and metals even when using a spray coating of silicone "mold release" the molds had to be made of a low melting material.³ Paraffin was found to be an excellent mold material particularly from the standpoint of preventing casting stresses. However, its use as the mold material necessitated machining of all castings due to surface imperfections and required care to prevent its melting during the heat release stage of the reaction. Further experimenting disclosed that aluminum foil between the plastic and the paraffin reduced the surface imperfections due to paraffin alone; yet the aluminum foil was easily peeled off the hardened casting.

The calibration specimens were cast in paraffin molds open at the top and since they were small, the heat release was insufficient to melt the mold.

The models were fabricated from two cast cylinders machined and cemented to form a "size-on-size" tee connection. Three models were fabricated in all. In each case they were prepared from two cylinders rather than by casting as a single unit due to the need for machining outer as well as inner surfaces.

The first tee was prepared from cylinders whose outside molds were aluminum foil tubes reinforced with paraffin. These outside molds were prepared by wrapping aluminum foil around a mandrel and then building up the paraffin coating by dipping into a vat of melted paraffin and removing. This was done in the manner of preparing a chill casting. After a

3. It is recommended that in future studies involving the casting of models from epoxy resins, further attention be given to the possibility of obtaining suitable mold release compounds.

sufficiently thick layer of paraffin was built up and allowed to harden the mandrel was removed and the aluminum foil was retained in place by the paraffin. The cores for these cylinders were solid paraffin. The mixed plastic was then poured into the mold from the open end. After the plastic hardened, the outer paraffin was easily pulled off and the aluminum foil peeled off; then the core was melted out and the cylinders were ready for machining.

The second tee had the same type of outside mold; however, the cores were glass cylinders wrapped with aluminum foil. In this case after hardening, the glass cylinder was pulled out and the aluminum foil was peeled off the inner surfaces of the cast cylinder.

The cylinders for the third tee had outer molds of basically the same idea except that the chill casting coating of paraffin was replaced by allowing the aluminum foil wrapped mandrel to solidify in a tall container of melted paraffin and then removing the mandrel. The cores for these cylinders were metal tubing wrapped with aluminum foil. After hardening, moderate warming freed the cast cylinder from the paraffin and then the aluminum foil was peeled off as before. Similarly the metal tubing was pulled free and the inner aluminum foil peeled off.

In the latter two cases the generous wrapping of aluminum foil around the glass or metal core provided for shrinkage and the glass or metal was easily removed.

2. Cementability.

The ability to produce the more complicated models needed in three-dimensional photoelasticity may well depend upon fabricating them by cementing. In this investigation the tee connections were prepared by

cementing two cylinders together. The cement used was the same Armstrong C-9 adhesive in the same proportions. It was first applied in thin coats to both surfaces to be joined then the surfaces were placed in close contact and held with only sufficient pressure to prevent relative movement during hardening. Figure 13 shows a circular disk subjected to concentrated diametrical loads and for comparison, Figure 14 shows the same disk after cementing subjected to the same loading. As may be seen the resulting stress pattern shows little or no disturbance at the cemented joint.

The frozen stress pattern in a slice from the third tee is shown in Figure 15 and again it shows negligible disturbance at the cemented joint. It was found that the disturbance of a cemented joint increased as the thickness of the glue line increased. In cementing a joint by butting, the parts to be joined were held $1/16$, $1/8$, and $1/4$ " apart and this space was then filled with the plastic and upon observance of the joint under loading showed a radical change in the stress pattern. The type of bonding in this cementing is of the adhesive type and the tensile strength of the bonded joint was in all cases nearly equal to that of a solid piece. The strength of a butt joint, however, was observed to be greatly decreased for loading imposing bending and shear upon the joint.

In the fabrication of the tee connections the manner was varied in each case. The first tee was constructed by boring the header to receive the branch. After cementing, the portion of the branch protruding inside the header was removed by boring. In the second and third tees the header remained whole and the end of the branch was formed to a saddle shape and cemented to the header. The variations in the second and third tees, however, was the thickness of the glue line. In the second, it was

approximately $1/16''$ to $1/8''$, whereas in the third tee, it was a minimum thickness. The frozen stress pattern at a cemented joint of minimum glue line thickness gave a very negligible distortion as shown in Figure 15, whereas the thicker glue line produced radical distortion. After curing, the boring through the header wall was accomplished through the branch end. Figure 12 shows the third tee after cementing and with the dimensions of Figure 16.

As shown in Figure 17, the cementing produced a joint that looked very similar to the actual joint produced by welding in the fabrication of a piping tee connection. This is considered noteworthy in justifying the use of three-dimensional photoelasticity as a means of analyzing the stress distributions in a piping tee connection.

3. Machining.

The machining properties of Armstrong's C-9 adhesive were found to be very good. Ordinary metal working lathes and milling machines were employed and although machining stresses were introduced they were easily annealed out by soaking at the critical temperature for several hours and very slowly cooling. Hand filing, sanding, and power grinding (parallel surfacing) were other low machining stress inducers; however, power sanding was unsatisfactory from this standpoint. Normal metallurgical polishing methods produced excellent results, but were not used on the final model slices since they were so slow.

As mentioned earlier, brittleness of Armstrong's C-9 adhesive was apparent only when castings were poured after too long a pot life.

4. Difficulties Encountered.

The combination of bubbles and soft spots in castings was of continual harassment to the writer. These are not considered to be a peculiar fault of Armstrong's C-9 adhesive but rather difficulties that the investigator had to experience, appreciate, and attempt to overcome.

The soft spots were particularly discouraging since they were not discovered until machining and then in what to all other respects appeared to be a sound casting.

The ability to repair the larger bubbles and soft spots was a definite assist in completing the tee connections. The bubbles were drilled out and then filled with the plastic using aluminum foil to hold it in place. The soft spots when uncovered in the machining were scraped until all the unhardened plastic was removed then the area was covered with new plastic.



FIGURE 11. Header and Branch of Third Tee Prior to Cementing.



Figure 12. Third Tee After Cementing.



FIGURE 13. Stress Pattern of a Circular Disk Under Load.



Figure 14. Stress Pattern of a Cemented Circular Disk Under Load.

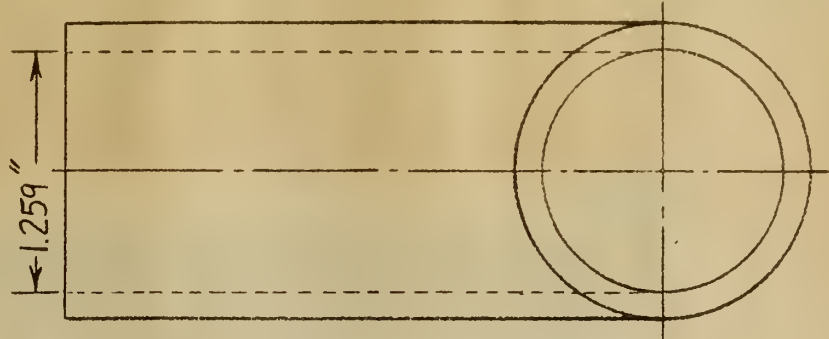
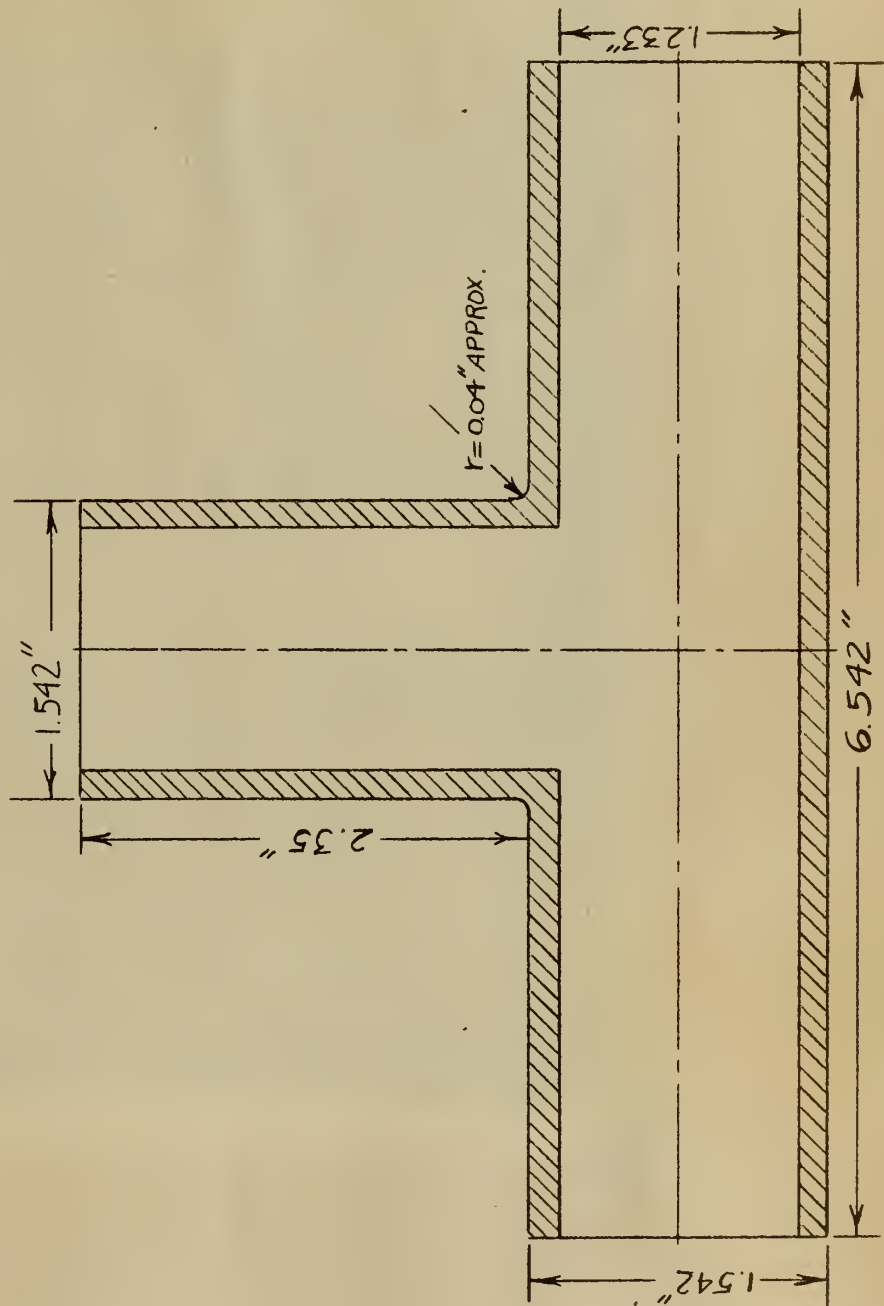
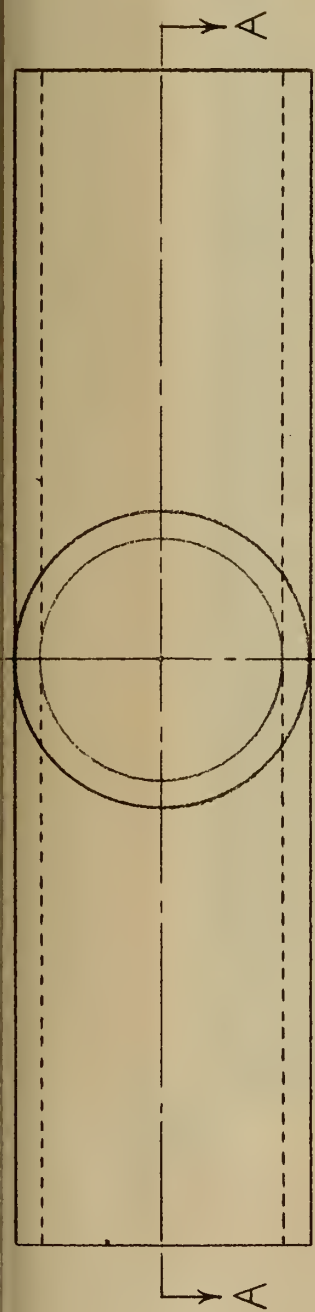


Figure 16. Details of Third Tee.



Figure 17. Similarity of Cemented Joint to a Welded Joint.

CHAPTER IV

TEST SET-UP AND PROCEDURE

The stress freezing apparatus was the essence of simplicity as shown in Figure 18. Hydrostatic loading was accomplished by means of a dead weight gage tester.⁴ The pressure was easily held constant by hand control of the tester.

The tee connections were blanked off at the header ends by casting in a plug of the plastic itself. Figure 19 shows the blanking off of one of the header ends of the third tee by means of a trough through the branch end. The closure of the branch end then was made by casting in a length of 1/4" piping for connecting to the pressure line. The completed third tee is shown in Figure 20. The tee was then filled with mineral oil and placed in the oven⁵ in wooden saddles as end supports. Brass weights were placed in the oven to maintain a slower rate of temperature change. After connecting up to the pressure line the heating was commenced without application of loading. The arrangement in the oven is shown in Figure 21. A typical heating and cooling cycle is shown in Figure 22.

Upon reaching the critical temperature the loading was applied to give a predetermined hoop stress from thin wall cylinder theory. The stress-strain curves of Figure 2 were utilized along with a safety factor of one-half to keep from stressing the juncture beyond the yield point. The time of holding the critical temperature was thirty minutes after which the temperature was lowered as shown in Figure 22 while maintaining constant loading. Figure 23 shows the test set up for the third tee including the pure bending specimen used for calibration purposes.

4. Lunkenheimer Dead Weight Pressure Gage Tester, 300 psi.

5. Central Scientific Company, Constant Temperature Oven.



Figure 18. Stress Freezing Apparatus.



Figure 19. Blanking Off the Ends of the Third Tee.



Figure 20. Third Tee Blanked Off and Ready for Testing.



Figure 21. Arrangement of Tee in the Oven.

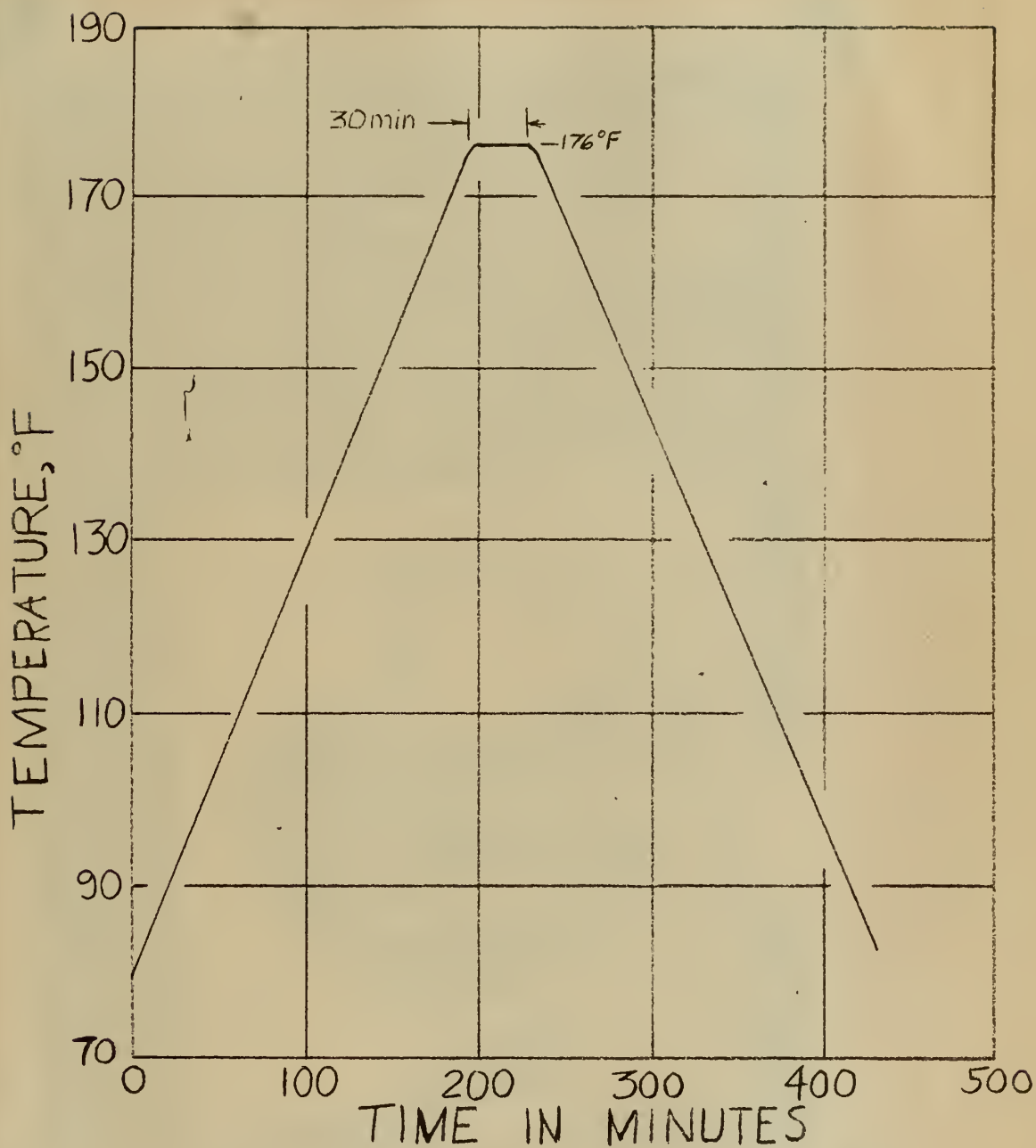


Figure 22. Stress Freezing Heating and Cooling Cycle.



Figure 23. Test Set-Up for Third Tee.

CHAPTER V

TEST RESULTS

1. Slicing.

Due to the low critical temperature of Armstrong's C-9 adhesive, extreme care must be exercised in slicing so as not to remove or disturb the frozen stress pattern. Several slicing operations were conducted to determine the best means of slicing.

The milling machine with slitting saws of 0.005" to 1/32", various cutting speeds, and with the feed of 1/2" per minute did not remove the pattern but gave such distortion that the slices had to have at least 1/16" excess on each side which then had to be removed by hand filing and sanding. The same result was found with the hand electric vibrating (Moto) saw and the electric jig saw.

The method that was found very satisfactory was by hand sawing using a hack saw with a blade of 32 teeth per inch. This method, however, was only satisfactory in the presence of a compressed air blast directed at the cutting point or, after the blade penetrated the tee, by having the air pass into the tee through the 1/4" fitting in the end of the branch and then out through the opening made by the cutting blade.

2. Interpretive Procedures.

In analyzing the slices in the polariscope shown in Figure 24 the slices were obtained from planes of symmetry. After eliminating the saw marks by hand sanding a uniform thickness⁶ was obtained to ± 0.001 " by

6. It should be noted that when using the stress freezing technique it is essential to maintain uniform thickness of a slice. In the more customary technique of observing plane stress models under load, variations in model thickness are not critical.

checking the thickness with a micrometer and sanding additionally the thick spots found. The slice was then immersed in a mineral oil bath for viewing thereby eliminating the necessity of polishing the specimen.

Since the main longitudinal centerline slice coincided with a plane of symmetry (of both loading and geometric shape) and thus a plane of known principal stress direction, this slice was chosen for examination. Due to the extended size of the slice it was necessary to photograph it in two parts as shown in Figures 25 and 26. The frozen stress pattern observed from this slice represents the relative retardation of the light rays due to the difference of principal stresses σ_z and σ_r expressed as $\sigma_z - \sigma_r = nF$. The identification of fringe orders was accomplished by counting from the zero order, the zero order being determined by examination of the slice in white light. White light examination was also useful in checking the fringe orders by observing color sequence.

Utilizing the known boundary conditions, σ_z was determined from the above relation. The variation of σ_z on the inner and outer surfaces of the branch along this plane of symmetry is shown plotted in Figure 27. The variation of σ_z on the inner and outer surfaces of the header along this plane of symmetry is shown plotted in Figure 28. The same results are tabulated in the appendix.

3. Static Checks.

Branch

$$(\sigma_z - \sigma_r)_{\text{outer}} = nF = 4 \times 10.55 = 42.25 \text{ psi}$$

$$\text{but } \sigma_r = 0, \text{ therefore } \sigma_z = 42.25 \text{ psi}$$

$$(\sigma_z - \sigma_r)_{\text{inner}} = nF = 5.5 \times 10.55 = 58.1 \text{ psi}$$

$$\text{but } \sigma_r = -17.5 \text{ psi, therefore } \sigma_z = 40.6 \text{ psi}$$

Hence $(\sigma_z)_{avg.} = [(\sigma_z)_{inner} + (\sigma_z)_{outer}]/2 = 41.43 \text{ psi}$

Area of branch wall = $\frac{\pi}{4} [(1.5585)^2 - (1.3015)^2] = .5685 \text{ sq.in.}$

Force in branch wall = $41.43 \times .5685 = 23.5 \text{ lbs.}$

Force in branch wall due to loading = $\frac{\pi}{4} \times 17.5 \times (1.3015)^2 = 23.3 \text{ lbs.}$

Header

$(\sigma_z - \sigma_h)_{outer} = nF = 2.75 \times 12.35 = 34 \text{ psi}$

but $\sigma_h = 0$, therefore $\sigma_z = 34 \text{ psi}$

$(\sigma_z - \sigma_h)_{inner} = nF = 4.5 \times 12.35 = 55.6 \text{ psi}$

but $\sigma_h = -17.5 \text{ psi}$, therefore $\sigma_z = 38.1 \text{ psi}$

Hence $(\sigma_z)_{avg.} = 36.05 \text{ psi}$

Area of header wall = $\frac{\pi}{4} [(1.562)^2 - (1.282)^2] = .624 \text{ sq.in.}$

Force in header wall = $36.05 \times .624 = 22.5 \text{ lbs.}$

Force in header wall due to loading = $\frac{\pi}{4} \times 17.5 \times (1.282)^2 = 22.5 \text{ lbs.}$

4. Why the Complete Solution Was Not Attained.

The accomplishments to this point only set the stage for the complete solution of a piping branch connection subjected to internal pressure. Unfortunately they were so time consuming that the complete analysis could not be undertaken. In lieu thereof the partial analysis and static checks mentioned above were completed to substantiate the validity of the process of experimentation and analysis. Additional "slices" were removed and photographed as a matter of record and possible subsequent analysis for the complete solution. These additional "slices" and their identification are shown in Appendix III.



Figure 24. Polariscope Used in Analyzing Frozen Stress Patterns.

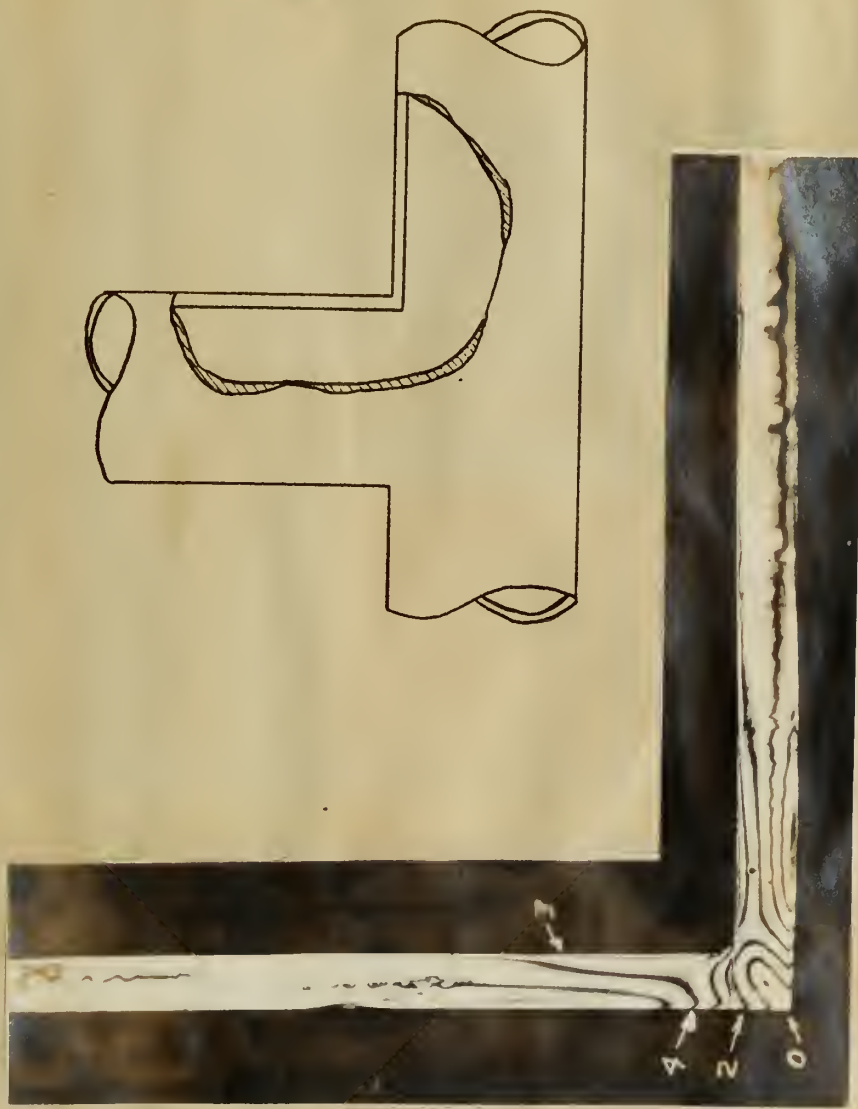


Figure 25. Partial View of Centerline Slice Used to Determine Longitudinal Boundary Stresses in Branch.

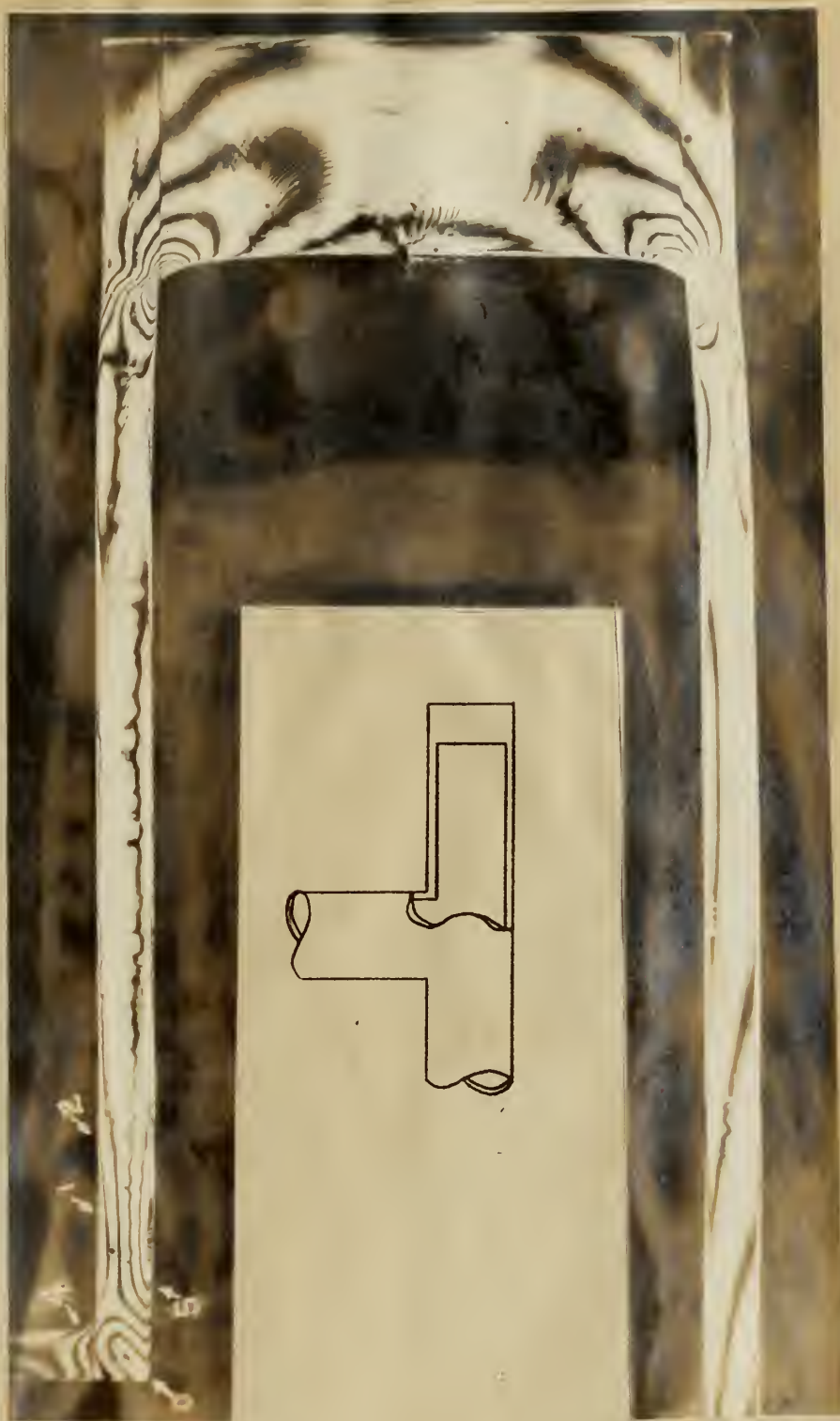


Figure 26. Partial View of Centerline Slice Used to Determine Longitudinal Boundary Stresses in Header.

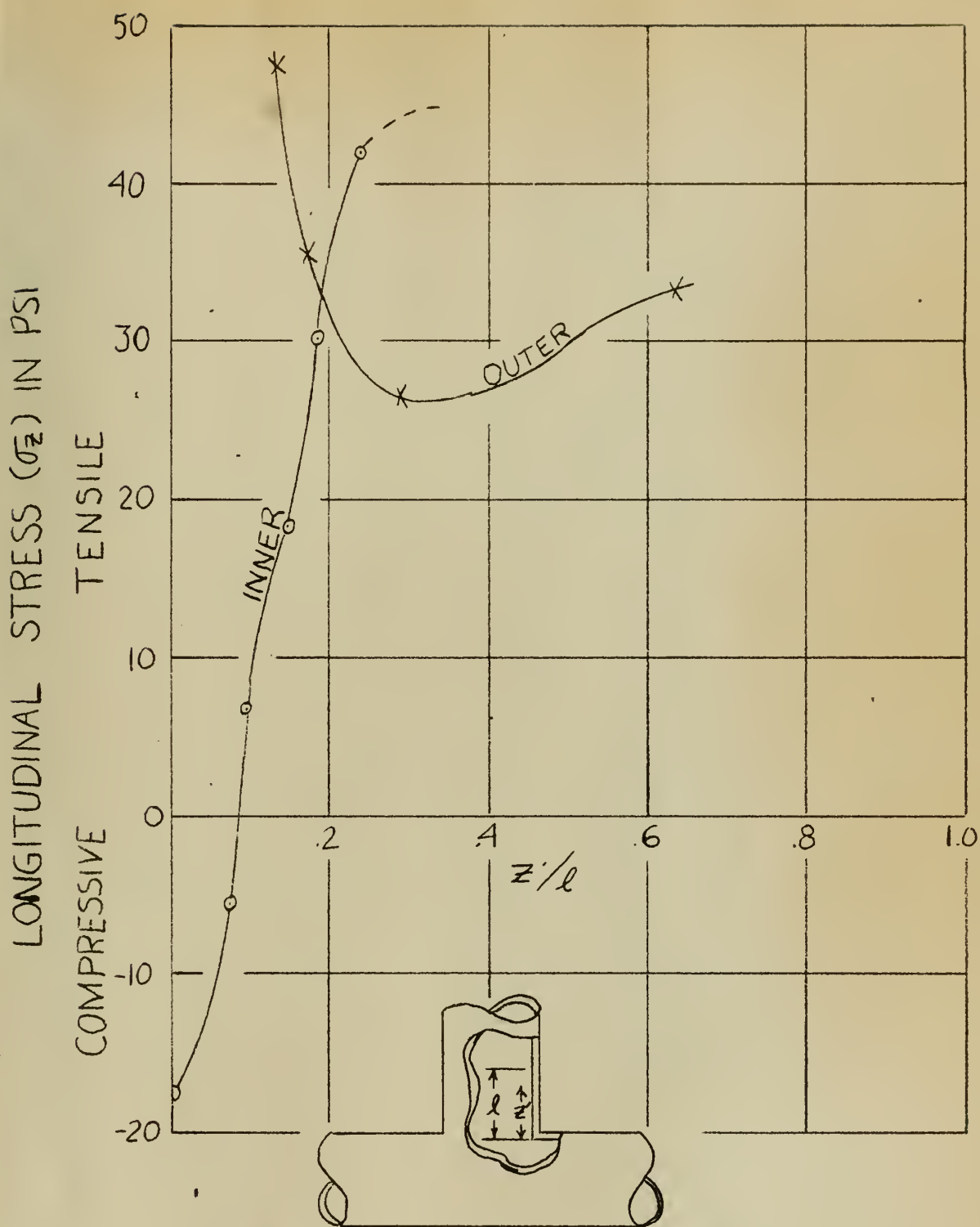


Figure 27. Plot of σ_z on Inner and Outer Surfaces Along Centerline of Branch.
 z' = axial distance measured on photograph, in.
 $l = 2.75''$

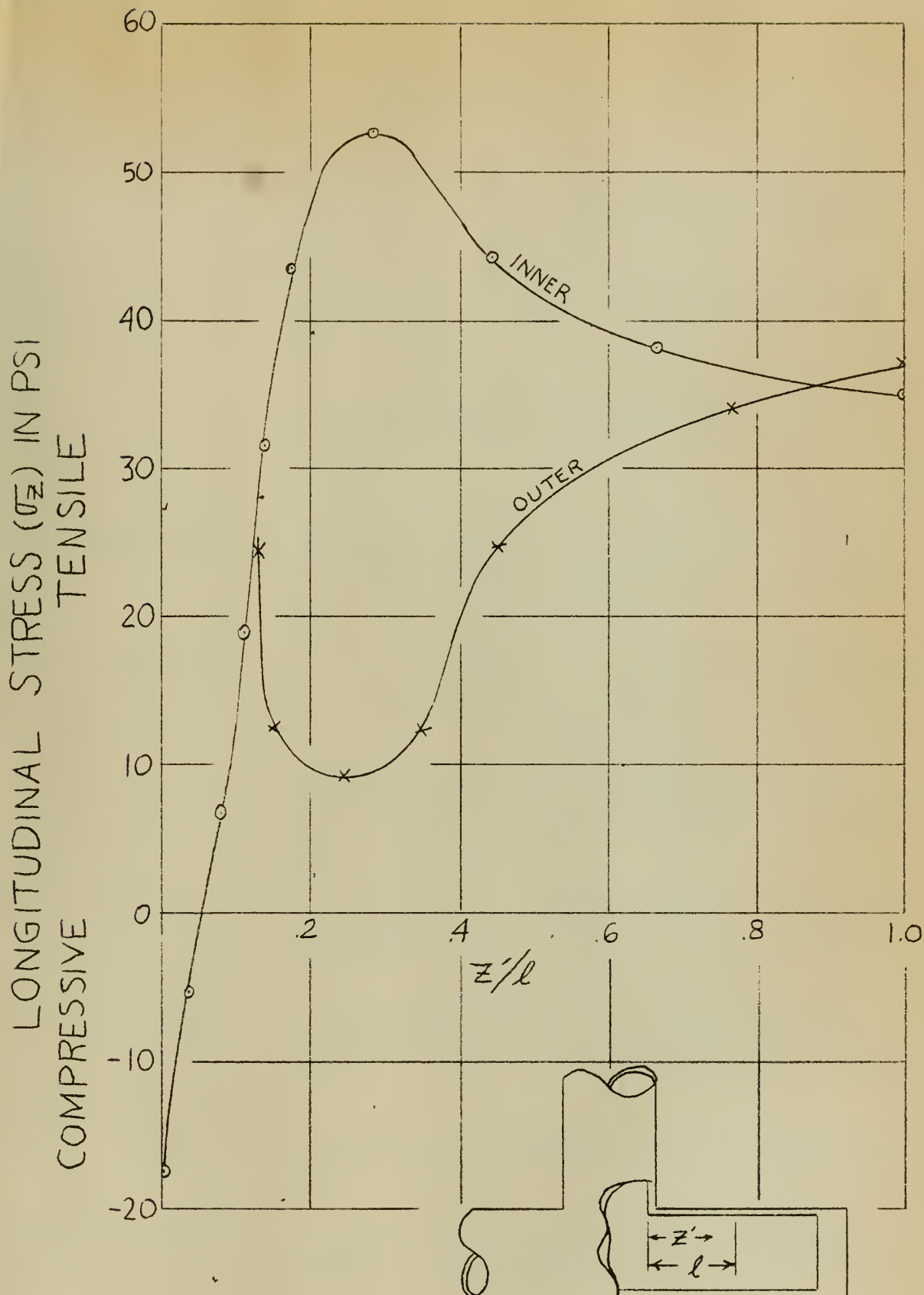


Figure 28. Plot of $\sqrt{\sigma_z}$ on Inner and Outer Surfaces Along Centerline of Header.
 z' = axial distance measured on photograph, in.
 l = 3"

BIBLIOGRAPHY

1. ASME BOILER AND PRESSURE VESSEL CODE, PART I, POWER BOILERS, Para. P-268 (1954 Addenda to 1952 Edition); PART VIII, UNFIRED PRESSURE VESSELS, Para. UG-36 to UG-46 inclusive, 1952 edition.
2. ASA B31.1-1951 and ASA B31.1a-1953, American Standard Code for Pressure Piping and Supplement No. 1, to same.
3. MAY 25, 1954 DRAFT (with revisions to November 17, 1954) OF PROPOSED DRAFT OF REVISION TO CHAPTER 5 OF SECTION 6 OF THE CODE FOR PRESSURE PIPING ASA B31.1.
4. M. M. Frocht & R. Guernsey, Jr. STUDIES IN THREE-DIMENSIONAL PHOTOELASTICITY - THE APPLICATION OF THE SHEAR DIFFERENCE METHOD TO THE GENERAL SPACE PROBLEM. Proceedings of the First U. S. National Congress of Applied Mechanics, December, 1952, pp. 301-307.
5. M. M. Frocht & R. Guernsey, Jr. A SPECIAL INVESTIGATION TO DEVELOP A GENERAL METHOD FOR THREE-DIMENSIONAL PHOTOELASTIC STRESS ANALYSIS, NACA Technical Note 2822, December, 1952.
6. H. T. Jessop THE DETERMINATION OF THE SEPARATE STRESSES IN THREE-DIMENSIONAL STRESS INVESTIGATIONS BY THE FROZEN STRESS METHOD. Journal of Scientific Instruments and of Physics in Industry, Vol. 26, 1949, pp. 27-31.
7. M. M. Leven A NEW MATERIAL FOR THREE-DIMENSIONAL PHOTOELASTICITY. Proceedings, S.E.S.A., Vol. VI, No. 1, 1948, pp. 19-28.
8. L. W. Smith AN INVESTIGATION OF DISCONTINUITY STRESSES IN PRESSURE VESSELS BY MEANS OF THREE-DIMENSIONAL PHOTOELASTICITY. Purdue University Thesis, August 1952.
9. C. E. Taylor DEVELOPMENT OF A NEW CASTING MATERIAL FOR THREE-DIMENSIONAL PHOTOELASTICITY. Purdue University Thesis, June 1948.
10. M. M. Frocht A NEW CEMENTABLE MATERIAL FOR TWO- AND THREE-DIMENSIONAL PHOTOELASTIC RESEARCH. Proceedings, S.E.S.A., Vol. XII, No. 1.

APPENDIX I

MECHANICAL PROPERTIES DATA

ROOM TEMPERATURE STRESS-STRAIN

Load lbs.	Δl .0001"	ϵ " / " $\times 10^{-5}$	σ psi
0	0	0	0
10	5	25	156
20	11	55	313
25	15	75	391
30	18	90	470
40	23	115	626
50	30	150	783
60	35	175	939
70	41	205	1094
75	45	225	1173
80	48	240	1251
90	53	265	1408
100	61	305	1562
110	65	325	1720
125	70	350	1955

$$\sigma = E \epsilon$$

$$E = \frac{\sigma}{\epsilon} = \frac{700}{132.5} \times 10^5 = .5275 \times 10^6 \text{ psi}$$

STRESS-STRAIN AT 78°C

ΔP grams	Total P grams	Δl .001"	Total Δl .001"	ϵ " / " $\times 10^{-3}$	Total P lbs.	σ psi
3.54	3.54	.4	.4	.2	.00783	3.58
5.00	8.54	1.2	1.6	.8	.01885	8.62
5.00	13.54	2.2	3.8	1.9	.0299	13.68
7.08	20.62	5.1	8.9	2.45	.0455	20.8
10.00	30.62	8.5	17.4	8.7	.0676	30.9
10.00	40.62	8.6	26.0	13.0	.0898	41.05
14.16	54.78	11.4	37.4	18.7	.121	55.35
20.00	74.78	19.7	57.1	28.55	.165	75.5
23.61	98.39	27.1	84.2	42.1	.2175	99.5
23.66	122.05	27.7	111.9	55.95	.270	123.3
24.06	146.11	36.5	148.4	74.2	.323	147.6
24.1	170.21	40.0	188.4	94.2	.377	172.3
24.34	194.55	37.0	225.4	112.7	.430	196.6

WIDTH = .247"

THICK. = .130"

TEMP. = 78°C

 σ = 457P

$$\sigma = \frac{P \times 14.7}{\text{Area}} = \frac{14.7}{(.247)(.13)} P = 457P$$

STRESS-STRAIN AT 87°C

ΔP grams	Total P grams	Δl .001"	Total Δl .001"	ϵ $\frac{1}{2}$ "/" $\times 10^{-3}$	Total P lbs.	σ psi
3.54	3.54	2.5	2.5	1.25	.00783	3.88
5	8.54	6.1	8.6	4.3	.01885	9.36
5	13.54	6.9	15.5	7.75	.0299	14.85
7.08	20.62	10.0	25.5	12.75	.0455	22.6
10	30.62	15.3	40.8	20.4	.0676	33.6
10	40.62	15.2	56.0	28.0	.0898	44.6
14.16	54.78	24.8	80.8	40.4	.121	60.1
20	74.78	34.6	115.4	57.8	.165	82.0
23.3	98.08	38.1	153.5	76.75	.2165	107.3
23.4	121.48	34.5	188.0	94.0	.2685	133.3
23.6	145.08	0	188.0	94.0	.321	159.4
24.0	169.08	0	188.0	94.0	.374	185.6
24.1	193.18	0	188.0	94.0	.426	211
25.5	218.68	0	188.0	94.0	.482	239
28.35	247.08	1	189.0	94.5	.546	271
33.5	280.53	27	216.0	108.0	.620	308

WIDTH = .2465"
 THICK. = .120"
 TEMP. = 87°C
 σ = 497P

STRESS-STRAIN AT 84°C

ΔP grams	Total P grams	Δl .001"	Total Δl .001"	ϵ " / " $\times 10^{-3}$	Total P lbs.	σ psi
5	5	1	1	.5	.0111	6.03
5	10	1	2	1	.0222	12.1
5	15	4	6	3	.0333	18.1
7.08	22.1	4.5	10.5	5.2	.049	26.6
10	32.1	10.5	21	10.5	.071	38.5
10	42.1	12	33	16.5	.093	50.4
10	52.1	12	45	22.5	.115	62.4
14.16	66.3	20	65	32.5	.145	78.6
10.3	76.6	15	80	40.0	.169	91.6
10.5	87.1	16	96	48	.193	104.8
10.5	97.6	13.5	109.5	54.7	.216	117
17.5	114.7	30.5	140	70.0	.253	137
17.2	131.9	25	165	82.5	.291	158
17.45	149.4	26	191	95.5	.330	179
17.60	167.0	25	216	108.0	.369	200
18.18	185.2	-1	215	107.5	.408	221
18.35	203.6	1	216	108.0	.448	243
20	226.9	3	219	109.5	.493	267

WIDTH = .251"
 THICK. = .108"
 TEMP. = 84°C
 LEVER ARM = 14.7

$$\sigma = \frac{Px \text{ lever}}{\text{Area}} = \frac{14.7}{(.251)(.108)} P = 542P$$

CREEP TEST AT 76°C

hr.	TIME		δ .001"
	min.	sec.	
16	40	00 (start of test)	0
	45	00	31
	50	00	66
	55	00	86
17	00	00	101
	05	00	112
	10	00	121
	15	00	129
	20	00	135
	25	00	141
	30	00	146
	35	00	150
	40	00	154
	45	00	157
	50	00	160
	55	00	162
18	00	00	163
	05	00	163.6
	10	00	164.0
19	00	00	166.2
20	00	00	167.3
21	15	00	168.1
21	30	00	168.2

$\bar{\sigma} = 169 \text{ psi}$

APPENDIX II

σ_z COMPUTATION DATA

P = 17.5 psi

f = 1.31 psi/in/fringe

BRANCH INNER

n	z' (")	z'/l	w (")	$F=f/w$	$\sigma_z - \sigma_r = nF$	σ_r (psi)	σ_z (psi)
0	0	0	.108	12.12	0	-17.5	-17.5
1	.12	.074	.108	12.12	12.12	-17.5	- 5.38
2	.23	.087	.108	12.12	24.24	-17.5	+ 6.74
3	.40	.149	.110	11.90	35.7	-17.5	+18.2
4	.50	.185	.110	11.90	47.6	-17.5	+30.1
5	.66	.240	.110	11.90	59.5	-17.5	+42.0

BRANCH OUTER

4	.38	.138	.110	11.90	47.6	0	47.6
3	.46	.1675	.110	11.90	35.7	0	35.7
2.25	.8	.29	.111	11.8	26.6	0	26.6
3	1.35	.636	.118	11.1	33.3	0	33.3

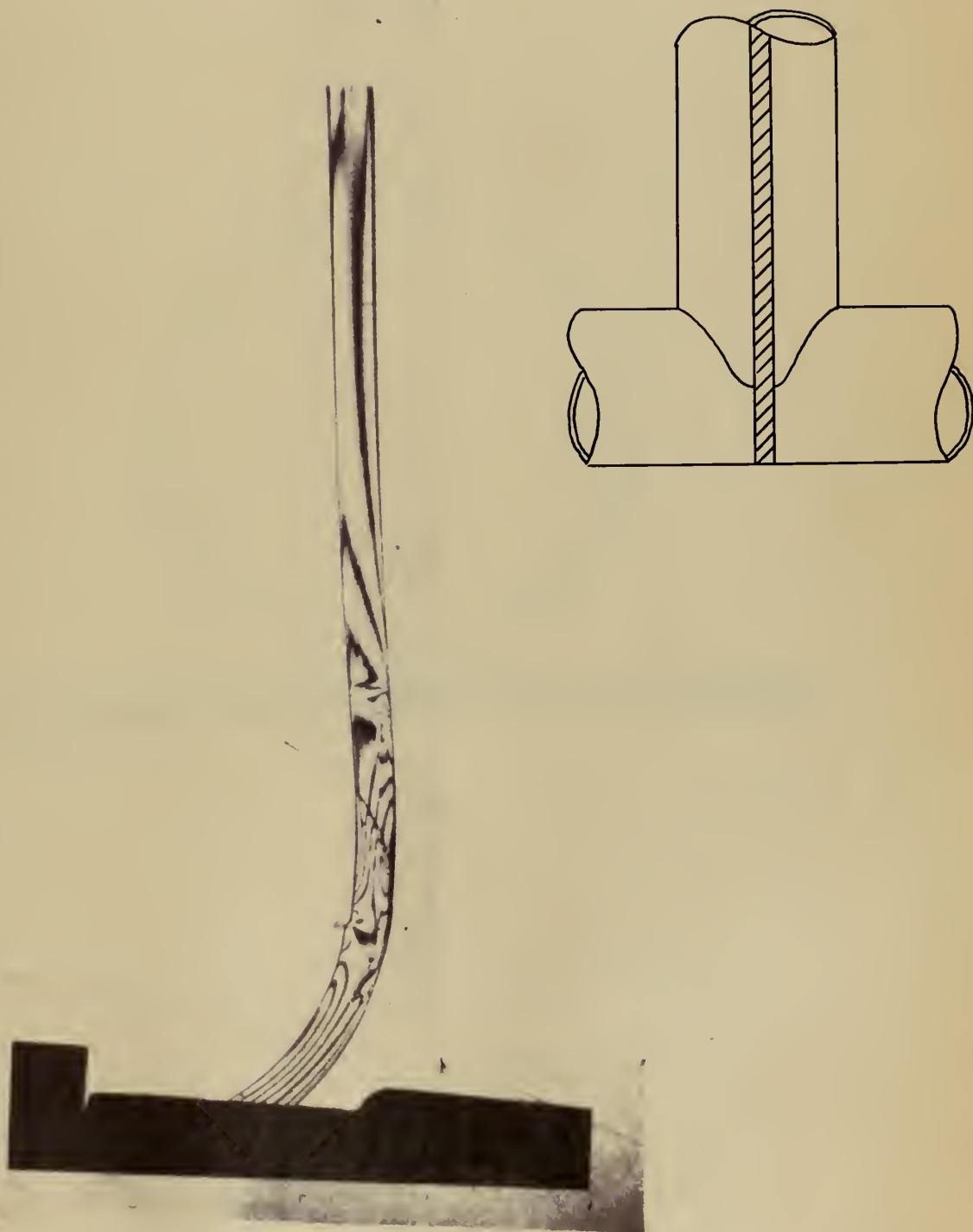
HEADER INNER

n	z' (")	$z'/1$	w (")	$F = f/w$	$\sigma_z - \sigma_z = nF$	σ_z (psi)	σ_z (psi)
0	0	0	.108	12.12	0	-17.5	-17.5
1	.11	.0367	.108	12.12	12.12	-17.5	- 5.38
2	.24	.08	.108	12.12	24.24	-17.5	+ 6.74
3	.33	.11	.108	12.12	36.4	-17.5	18.9
4	.42	.14	.1072	12.2	48.8	-17.5	31.3
5	.53	.176	.1072	12.2	61.0	-17.5	43.5
5.75	.85	.283	.1072	12.2	70.2	-17.5	52.7
5	1.34	.446	.106	12.35	61.7	-17.5	44.2
4.5	2.0	.666	.106	12.35	55.6	-17.5	38.1
4.25	3.0	1.000	.106	12.35	52.5	-17.5	35.0

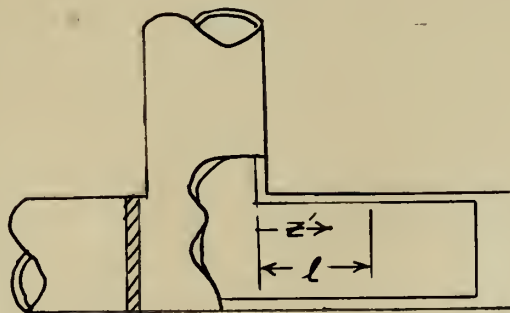
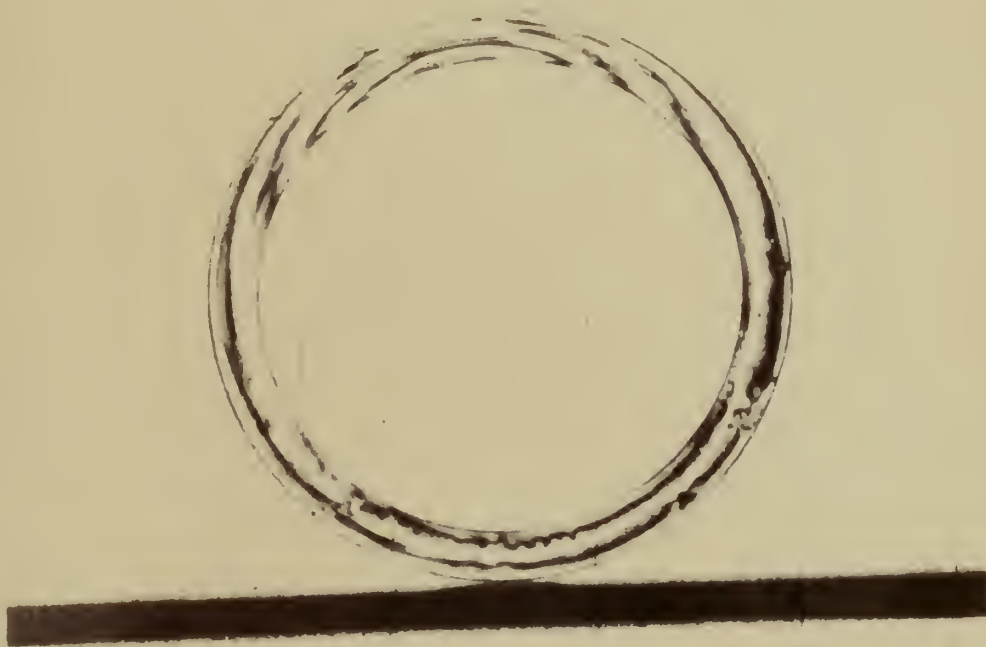
HEADER OUTER

2	.39	.13	.108	12.12	24.24	0	24.24
1	.45	.15	.108	12.12	12.12	0	12.12
.75	.75	.25	.1072	12.2	9.09	0	9.09
1	1.05	.35	.1072	12.2	12.12	0	12.12
2	1.35	.45	.106	12.35	24.70	0	24.70
2.75	2.3	.766	.106	12.35	34.0	0	34.0
3	3	1.000	.106	12.35	37.1	0	37.1

APPENDIX III



Transverse Slice Through Centerline of Branch



Transverse Slice Through Header at $z'/l = 0.104$

z' = axial distance measured on model, in.

$l = 1.43''$



FE 17 56

4 6 1 8

28481

Thesis
B8836

Burke

Photoelastic study of
pressure vessel stresses.

28481

Thesis

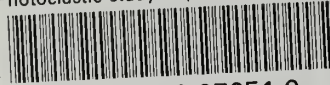
B8836

Burke

Photoelastic study of pressure
vessel stresses.

thesB8836

Photoelastic study of pressure vessel st



3 2768 002 07951 9

DUDLEY KNOX LIBRARY